Hindawi
Geofluids
Volume 2022, Article ID 1678442, 8 pages
https://doi.org/10.1155/2022/1678442

Research Article

Impact of Agricultural Use of Sand Land on Water Yield Services under Different Development Intensities in the Agro-Pastoral Ecotone of Northern Shaanxi

Yuan Xiu,[1] **Ni Wang**,[1] **Siyuan Liu**,[2] **Zihan Guo**,[1] **and Fangxu Peng**[1]

[1]*State Key Laboratory of Eco-Hydraulics in Northwest Arid Region, Xi'an University of Technology, Xi'an 710048, China*
[2]*College of Resources and Environment, Henan Agricultural University, Zhengzhou 450046, China*

Correspondence should be addressed to Ni Wang; wangni@xaut.edu.cn

Received 9 August 2022; Revised 16 September 2022; Accepted 24 September 2022; Published 12 October 2022

Academic Editor: Zhenlong Song

The impact of development on the ecological environment is a matter of concern, especially in the ecologically fragile agro-pastoral ecotone. The agro-pastoral ecotone of northern Shaanxi (ANS) is a representative region of the agro-pastoral ecotone in northern China. The agricultural use of sand land (AUSL) is an effective way to respond to the development needs of this region. The AUSL will certainly have an impact on water yield services in the ANS, where water resources are already scarce. In this study, the Integration Valuation of Ecosystem Services and Tradeoffs Tool (InVEST) model was used to simulate the water yield of the ANS under different intensity scenarios of AUSL. The results showed that AUSL reduces the regional water yield, but the impact is limited. At the maximum scale of development, the total regional water yield decreased by 1.35% compared to the base year of 2020. In terms of distribution pattern, water yield decreased the most in Yuyang District and the least in Fugu County due to the uneven distribution of sand land. At the land use and land cover (LULC) scale, the AUSL has a diminishing effect on the water yield of both cultivated land and sand land due to the more intense evapotranspiration from cropland. This study can provide data and decision support for the ANS region for building the resource-economical and environment-friendly society.

1. Introduction

Water resources not only play an indispensable and fundamental role in maintaining the normal functioning of ecosystems but also play a vital role in supporting human survival, social stability, and economic development [1–3]. However, the water crisis is becoming increasingly serious in today's society [4]. The increasing human demand for water resources, both quantitatively and qualitatively, has put unprecedented pressure on ecosystems to provide this service [5, 6], especially in arid regions [7, 8]. The reasons mainly come from two aspects: firstly, the urgent needs of development in arid regions have increased the pressure on water yield services; secondly, changes in the external environment such as climate and land use have seriously affected the stability of water yield services, which has formed a vicious circle with the already fragile ecological environment of the arid regions. Therefore, the study of the impact of development on water yield is an important tool to guarantee the sustainability of regional ecosystems and social systems, while safeguarding the right to the development in arid areas.

In arid regions, food production tends to be low due to constraints on soil and water resources, which has prompted more land to be reclaimed and a corresponding increase in water demand [9, 10]. In China, arid and semiarid areas account for nearly half of the country's land area [11], the area of cultivated land in arid and semiarid zones accounts for about 11.57% of the total area of cultivated land in the country. The agro-pastoral ecotone, a transitional zone where cultivated land and pastoral area intersect, has become the priority region for agricultural development. Thus, the treatment of sand land has also become a prerequisite for the development of agriculture.

Over the years, the paradigm of sand land management has shifted from passive management to active utilization. In the early stages, sand was mainly fixed by the methods of engineering [12, 13], biological [14], and chemical [15]. Nowadays, the integrated use model of "soilization" of sand land has become the main development direction, which takes into account the economic development while protecting the ecology. The essence of "soilization" is to improve the nutrient and moisture conditions of sandy soils for cultivation purposes by adding chemical amendments [16, 17], biological amendments [18], peat [19], processed plant residues [20], guest soil, or other natural raw materials [21] to the sand. The management model of sand land comprehensive utilization has been a useful exploration to curb the continuous reduction of cultivated land caused by urbanization and to adhere to the red line of cultivated land protection.

The agro-pastoral ecotone in northern Shaanxi (ANS) is a typical area of agro-pastoral ecotone in northern China. The northwest of ANS is the Mu Us Desert, and the southeast is the Loess Plateau. In addition, the entire area belongs to the Yellow River Basin. At the same time, the area is the focus of several national strategies or national policies, such as the Western Development Policy, the Loess Plateau Comprehensive Management Plan, and the major national strategy "Ecological Protection and High-Quality Development in the Yellow River Basin." In the last decade, urban expansion due to the rapid economic and social development in ANS has encroached on some agricultural land. Therefore, the agricultural use of sand land (AUSL) has become an effective way to alleviate the tight land resources and the increasing food demand in the region. The "soilization" of sand land has been proved feasible by many experts in the form of pilot experiments [22–24].

However, in order to achieve the goal of sustainable development, the development scale and the planting structure of AUSL in ANS are constrained by water resources. Water resource carrying capacity [25] and the strictest national water resource management system [26] are commonly used evaluation criteria for water resource constraints. Mathematical model optimization algorithms [27–29], system theoretical models, and hydro-physical models [30, 31] are appropriate tools for managing the scale and the structure of agricultural development under water constraints. In ANS, Liu et al. [32] have calculated the appropriate scale of agricultural development by developing the Water Resource Regulation-Allocation Coupling Model. The method can be described as follows: the maximum water quantity that can be used for agriculture in sand land can be calculated according to the limit conditions of total water resources, available water resources, available water resources of hydraulic engineering, and the total control index of the strictest national water resource management system; then, based on this upper limit, the planting scale and structure are optimized to maximize the benefits through the rational allocation of water. Although this study provides a reference threshold for the scale of AUSL in ANS, it did not conduct further research on the regional water yield service of LULC change from sand land to agricultural land.

As we all know, land use and land cover (LULC) change is one of the most important factors affecting hydrological processes. The water yield service is the most intuitive manifestation of this impact. Many studies have used models such as Hydrological Simulation Program Fortran (HSPF), MIKE SHE, TOPMODEL, Soil and Water Assessment Tool (SWAT), Modflow, and Integrate Valuation of Ecosystem Services and Tradeoffs Tool (InVEST) to quantitatively assess and evaluate the impact of LULC change on water yield. Among numerous models, the InVEST model, due to the advantages of fewer model parameters, lower data requirements, intuitive visualization of results, and high generality, has been widely used in the evaluation of ecosystem services including water yield [33–36]. This provides a suitable tool for assessing the water yield service of AUSL in the ANS.

Therefore, in this study, taking water yield as the representative indicator, the changes of water yield service under different development intensity scenarios of AUSL in ANS region were simulated by the Annual Water Yield module of the InVEST model. This study can provide a data reference for the impact of AUSL on the ecological environment and the sustainable development of ANS.

2. Materials and Methods

2.1. Study Area. Geographically, ANS belongs to the transition zone from the Loess Plateau to the Mu Us Desert and is an important part of the agro-pastoral ecotone in northern China. It is adjacent to Gansu Province and Ningxia Province in the south, connected to Inner Mongolia Autonomous Region in the north, and bounded by the Yellow River with Shanxi Province in the east. In terms of administrative division, there are two ways to divide the scope of the ANS [32, 37, 38]. Combined with the AUSL, this study adopts the division accepted by more scholars, which includes six counties (or districts) in the northern part of Yulin City, from west to east, namely, Dingbian, Jingbian, Hengshan, Yuyang, Shenmu, and Fugu. The geographical coordinates of the study area are between 36° 48′ and 39° 35′ N and 107° 14′ and 111° 08′ E, with a total area of 33,603.80 km^2, and the geographical location and administrative division of ANS are shown in Figure 1.

2.2. Scenario Description. Based on relevant studies, the upper limit of the development scale threshold for AUSL in the ANS by compounding arsenic sandstone with sand to form cultivated land can be described as follows: with normal water supply from all planned water conservancy projects, the sand land in the entire study area can be used as cultivated land except for 3434.51 ha of sand land which is not used in Yuyang [24, 32]. In this study, this threshold was also adopted as the upper limit of AUSL. Furthermore, the year 2020 was taken as the base year, and four scenarios were set up according to the different scales of AUSL to analyze the water yield service of AUSL in ANS. Scenario 1 was defined as the undeveloped mode, which is the base year of 2020. Scenario 2 was defined as 30% of the unused sand land in each county or district in the base year being developed

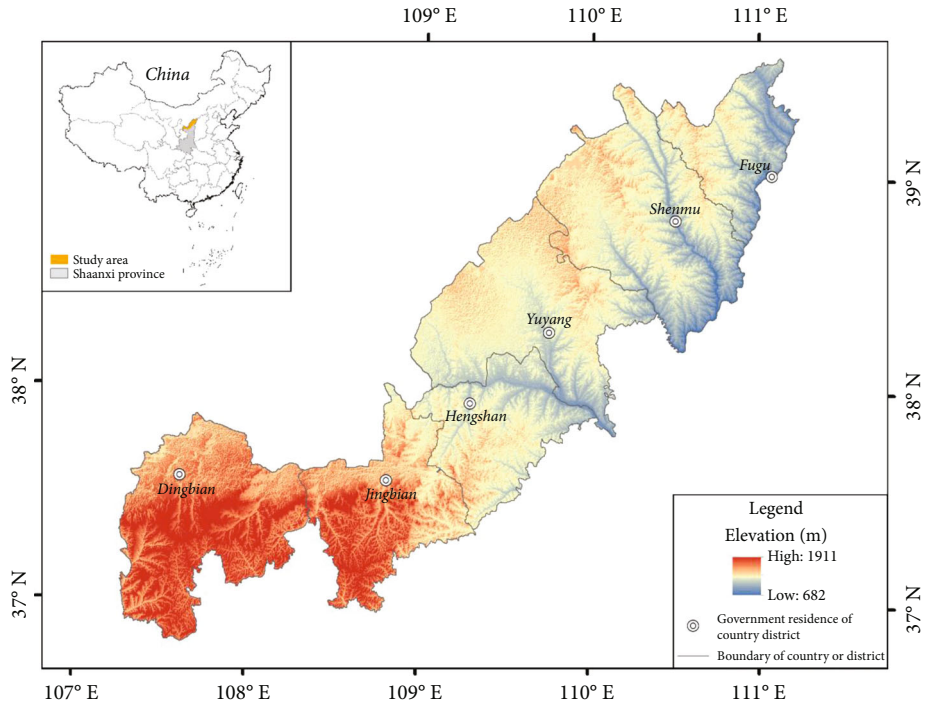

Figure 1: Location and elevation of the agro-pastoral ecotone of northern Shaanxi.

for cultivated land, that is, the low-intensity development mode. Scenario 3 is the medium-intensity development mode which can be described as 60% of the unused sand land being developed as cultivated land. Scenario 4 is the high-intensity development mode, that is, the development scale of the sand land reaches the upper limit. Table 1 shows the area of AUSL in different counties or districts under different scenarios.

2.3. Assessment of Water Yield. The annual water yield is derived from simulations with the InVEST model (version 3.11.0, Workbench). The annual water yield assessment module is based on the coupled hydrothermal equilibrium hypothesis proposed by Budyko in 1974 [39] and the average annual precipitation data for the work [34].

The water yield module of the InVEST model is based on the water balance principle, where the actual evapotranspiration is subtracted from the precipitation of each grid cell to obtain the amount of water produced by the grid. Instead of making a distinction between surface water, groundwater, and baseflow [40], the model assumes that the produced water in each grid cell can be pooled through each of these pathways. Thus, the model output is the total and average amount of water produced in the study area. Using the raster as the minimum calculation unit helps to distinguish the spatial heterogeneity of the yield sink, such as land use type, soil type, precipitation, and vegetation type. The model calculations are based on the following principles:

$$Y(x) = P(x) - \mathrm{AET}(x) = \left[1 - \frac{\mathrm{AET}(x)}{P(x)}\right] \times P(x), \quad (1)$$

Table 1: The developed area of sand land under different scenarios.

	Scenario 1 (ha)	Scenario 2 (ha)	Scenario 3 (ha)	Scenario 4 (ha)
Dingbian	0	13848.03	27696.06	46160.10
Jingbian	0	18362.21	36724.43	61207.38
Hengshan	0	12191.72	24383.43	40639.05
Yuyang	0	59882.54	119765.09	196173.97
Shenmu	0	23952.43	47904.86	79841.43
Fugu	0	330.99	661.99	1103.31
Total	0	128567.93	257135.85	425125.24

where $Y(x)$ is the water yield of grid x (mm), $\mathrm{AET}(x)$ is the actual annual evapotranspiration of grid x (mm), and $P(x)$ is the multiyear average precipitation of grid x (mm). For vegetated LULC in InVEST model, The evapotranspiration component of the water balance is usually associated with potential evapotranspiration (PET) [1], the calculation method is as follows [41, 42]:

$$\frac{\mathrm{AET}(x)}{P(x)} = 1 + \frac{\mathrm{PET}(x)}{P(x)} - \left[1 + \left(\frac{\mathrm{PET}(x)}{P(x)}\right)^{\omega}\right]^{1/\omega}, \quad (2)$$

where $\mathrm{PET}(x)$ is the potential evapotranspiration on pixel x and $\omega(x)$ is a nonphysical empirical fitting parameter.

$\mathrm{PET}(x)$ can be calculated from the following equation:

$$\mathrm{PET}(x) = K_c(l_x) \cdot \mathrm{ET}_0(x), \quad (3)$$

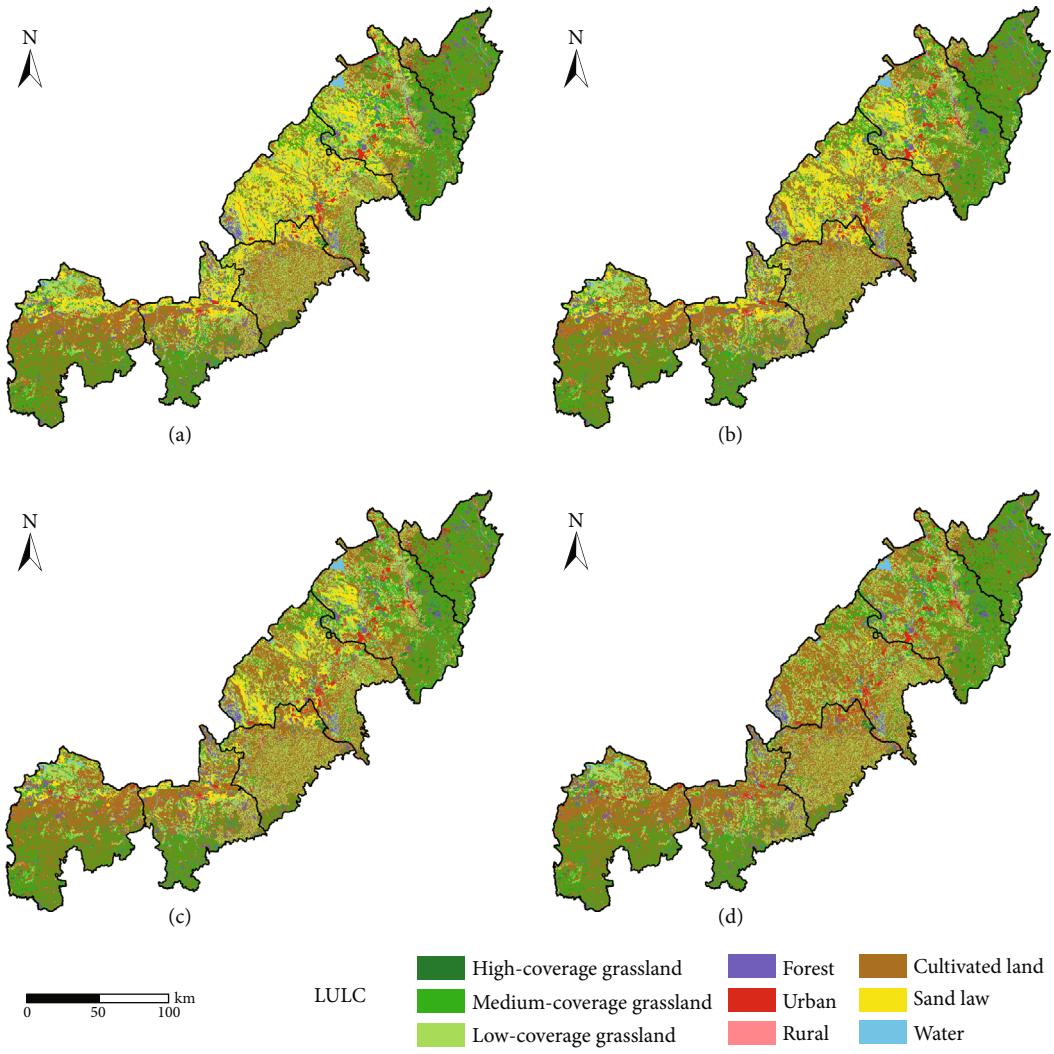

Figure 2: Classification LULC under different scenarios: (a) scenario 1; (b) scenario 2; (c) scenario 3; (d) scenario 4.

where $K_c(l_x)$ indicates the plant evapotranspiration coefficient for a specific LULC type in raster cell x. $ET_0(x)$ is the reference crop evapotranspiration, which is one of the model's input.

The $\omega(x)$ is a nonphysical empirical fitting parameter that characterizes the land surface properties including vegetation, climate, soil, and other factors. In InVEST model, the value of $\omega(x)$ is calculated following the approach of empirical formula [43]:

$$\omega(x) = Z\frac{\mathrm{AWC}(x)}{P(x)} + 1.25, \tag{4}$$

where Z is an empirical constant that characterizes the precipitation pattern and hydrogeological features and is usually taken in the range of 1 to 30 [44]. $\mathrm{AWC}(x)$ indicates the plant available water content (mm), which was influenced by the soil texture and effective soil depth. It is the total amount of water stored and provided by the soil during plant growth, determined by the plant available water content (PAWC), and the minimum value of the maximum soil root burial depth and the plant root depth, i.e.,

$$\mathrm{AWC}(x) = \mathrm{Min}(\mathrm{Layer.depth}, \mathrm{Root.depth}) \times \mathrm{PAWC}(x), \tag{5}$$

where Layer.depth and Root.depth represent the maximum root burial depth of the soil and plant root depth, respectively.

2.4. Data Sources. The Water Yield module of the InVEST model requires multiple types of raster datasets and parameters such as meteorology, vegetation, and geography as inputs to run. Precipitation data were obtained by kriging interpolation of monitored data from meteorological stations in and around the study area using Arcgis (10.4), which was obtained from the China Meteorological Data Service Centre (CMDC, http://data.cma.cn/). The reference crop evapotranspiration (ET_0) data was calculated according to the Penman-Monteith formula, the only

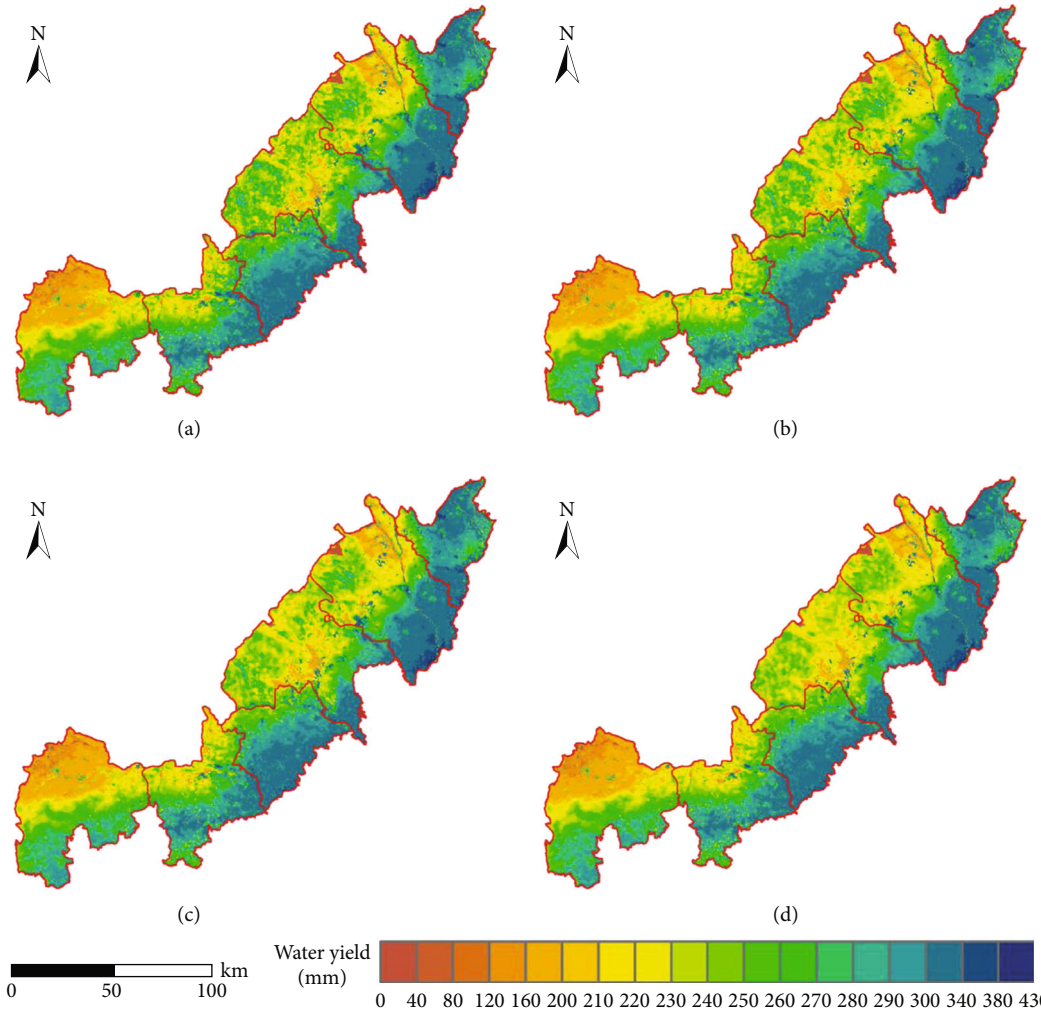

Figure 3: Changes in the spatial distribution of water yield under different development and utilization intensities: (a) scenario 1; (b) scenario 2; (c) scenario 3; (d) scenario 4..

method specified by the Food and Agriculture Organization of the United Nations (FAO). The data required for Penman-Monteith formula, such as temperature and radiation, were obtained from the monitoring data of various weather stations of CDMC (http://data.cma.cn/). Kriging interpolation is performed on the calculated data for each station to obtain the evapotranspiration raster data. Root depth and PAWC were obtained from the Harmonized World Soil Database (HSWD) provided by FAO. Land use/land cover was derived from the Resource and Environmental Science Data Center of the Chinese Academy of Sciences (http://www.resdc.cn). The resolution of all raster data was 30 m ∗ 30 m. Also, the projection coordinate system of all raster and vector data was WGS_1984_UTM, and the geographic coordinate system was GCS_WGS_1984.

3. Results and Discussion

3.1. LULC of Different Scenarios. According to the four scenario settings, the land use of the base year was edited using Arcgis10.4 software, and the land use corresponding to scenario 2~scenario 4 was obtained. In this study, the land use in the study area was divided into nine categories, which were high-coverage grassland, medium-coverage grassland, low-coverage grassland, forest, urban, rural, cultivated land, sand land, and water, as shown in Figure 2. In 2020, the base year, the area of sand land accounts for 12.75% of the total area of ANS and is mainly distributed in Yulin, Shenmu, and Jingbian of the study area. Yuyang District has the largest area of sand land, accounting for 28.87% of the total area of Yuyang District and 46.58% of the total area of sand land in ANS. The area of sand land in Fugu is the least, accounting for 0.35% of Fugu area and 0.26% of the total area of sand land.

3.2. Effect of AUSL on Water Yield

3.2.1. Variations in the Spatial Distribution of Water Yield. There are significant differences in water yield for different exploitation intensity scenarios, as shown in Figure 3. In general, there is spatial heterogeneity in water yield in the ANS region, showing a general pattern that the east is larger than the west and the south is larger than the north. Fugu in

Table 2: Changes in water yield of cultivated and sand land under different scenarios.

LULC	Scenario 1 Water yield (mm)	Scenario 2 Water yield (mm)	Scenario 3 Water yield (mm)	Scenario 4 Water yield (mm)
Cultivated land	264.05	261.11	259.01	256.04
Sand land	261.95	261.28	259.36	258.52

the northeast produces the largest amount of water, while Dingbian in the southwest produces the least. The water yield of each grid was within the range of 0 mm to 423.16 mm for all four scenarios. With the increase of development intensity, the water yield in the study area gradually decreases, and the corresponding water yields in the four scenarios are 260.46 mm, 259.38 mm, 258.41 mm, and 257.02 mm, respectively. As can be seen from Figure 3, the change in water yield distribution pattern in Yuyang and Shenmu is more pronounced.

3.2.2. Variation of Water Yield under Different Development Intensities. According to the principle of calculating water yield by InVEST, this study only needs to discuss the variation of water yield in sand and cultivated land. Table 2 shows the water yield of sand and cultivated land for the four scenarios. It can be found that the water yield of both sand and cultivated land is on a decreasing trend. For cultivated land, the water yield shows a trend of decrease because the additional cultivated land is converted from sand land, which is often located in areas with low rainfall, and also, the evapotranspiration coefficient of cultivated land is greater. As a large amount of sand land is developed for cultivation, the priority development of sand land is often the part of the land that is more suitable for precipitation and evaporation, which is the main reason for the decrease of water yield in sand land.

Table 3 shows the water yield of other types of LULC. This shows that water yield of urban is the largest, which is consistent with the conclusion obtained from most studies that urbanization leads to an increase in runoff [45, 46]. Although evaporation is greater in urban, there is also a trend towards more precipitation in urban, especially extreme precipitation events, which can explain this phenomenon well. Except for urban and waters, the remaining seven types of LULC yielded water in the range of 200 mm to 300 mm. The least water yield is the land covered by forest land, due to the higher potential evapotranspiration from the forest land [47]. Grasslands with high cover yield more water, which is closely related to the distribution of grassland: grassland with high cover is mostly located in areas with high precipitation and low evapotranspiration.

3.2.3. Changes in Total Water Yield. Table 4 shows the data for total water yield by county and for the ANS as a whole for the four scenarios. In terms of total water yield in the study area, the total water yield decreased by 0.44% when the development intensity was low, 0.81% when the development intensity was medium compared to the base year, and 118.11 million m^3 when the development intensity reached its maximum, a decrease of 1.35% compared to the base year. This is due to the fact that in the model, the evaporation coefficient is higher for cultivated land than for sand land, and the water yield decreases accordingly, all else being equal.

Table 3: Water yield of different types of LULC (excluding cultivated and sand land).

LULC	Water yield (mm)
High-coverage grassland	292.91
Medium-coverage grassland	274.91
Low-coverage grassland	250.72
Forest land	211.18
Urban	325.60
Rural	290.11
Water	73.55

Table 4: Changes in total water yield by administrative regions under different scenarios.

	Scenario 1 (10^6 m^3)	Scenario 2 (10^6 m^3)	Scenario 3 (10^6 m^3)	Scenario 4 (10^6 m^3)
Dingbian	1562.98	1558.29	1555.20	1547.99
Jingbian	1317.58	1311.35	1306.13	1299.55
Hengshan	1218.47	1212.41	1210.73	1205.91
Yuyang	1750.88	1734.96	1718.62	1698.82
Shenmu	1971.42	1966.21	1959.97	1951.65
Fugu	933.49	932.99	932.94	932.79
Total	8754.82	8716.21	8683.59	8636.71

Due to the less distribution of sand land in Fugu, the use of sand land as cultivated land has little impact on the total water yield in the region. So, the water yield is relatively stable, and the total water yield only decreases by 0.07% when the maximum development intensity is reached. The proportional changes in total water yield corresponding to Yuyang in scenarios 2, 3, and 4 are 0.91%, 1.84%, and 2.97%, which are the most affected among all county-level administrative regions. The reason is that nearly half of ANS's sand land is distributed in Yuyang. The ranking of the impact of different development intensities on each county was obtained according to the reduction in the total amount of water yield. The degree of impact under low development intensity is Yuyang > Hengshan > Jingbian > Dingbian > Shenmu > Fugu; the degree of impact under medium development intensity is Yuyang > Jingbian > Hengshan > Shenmu > Dingbian > Fugu; the ranking under high development intensity is Yuyang > Hengshan > Jingbian > Shenmu > Dingbian > Fugu in order.

4. Conclusions

Water yield service is crucial for ecologically fragile arid and semiarid areas, and changes in LULC can have an impact on

water yield services. This study quantitatively assessed the changes in water yield due to different development intensities of AUSL in ANS with the InVEST model using 2020 as the base year.

In general, with the increase in the area of AUSL, the water yield in ANS is on a downward trend, and the reduction of water yield under the maximum development intensity is 1.35% compared to 2020, which has less impact on regional water yield services. In terms of the spatial distribution pattern of water yield, since more than 40% of the sand land is distributed in Yuyang, the water yield service of Yuyang is the most affected, while Fugu is the least affected administrative region. From the LULC perspective, AUSL has a decreasing effect on the water yield of both cultivated land and sand land. In summary, it can be seen that AUSL in the ANS has a decreasing effect on regional water yield services, but to a limited extent. The results imply that the AUSL under the development intensity threshold is feasible provided that the planned hydraulic project is operating normally. This study can provide decision aid for the sustainable development of the region.

Data Availability

All data, models, and software generated or used during the study appear in the submitted article.

Conflicts of Interest

The authors declare no conflicts of interest.

Acknowledgments

This work was supported by the National Natural Science Foundation of China (grant no. 51979221), by the Natural Science Basic Research Program of Shaanxi (program no. 2021JLM-45), and by the Research Fund of the State Key Laboratory of Eco-hydraulics in Northwest Arid Region, Xi'an University of Technology (grant no. 2019KJCXTD-5).

References

[1] P. Wei, S. Chen, M. Wu et al., "Using the InVEST model to assess the impacts of climate and land use changes on water yield in the upstream regions of the Shule River Basin," *Water*, vol. 13, no. 9, p. 1250, 2021.

[2] M. V. Semenov, G. S. Krasnov, K. Y. Rybka et al., "Spatial changes in microbial communities along different functional zones of a free-water surface wetland," *Microorganisms*, vol. 8, no. 10, p. 1604, 2020.

[3] J. Tian, S. L. Guo, L. L. Deng et al., "Adaptive optimal allocation of water resources response to future water availability and water demand in the Han River basin, China," *Scientific Reports*, vol. 11, no. 1, 2021.

[4] L. G. Shen, Z. Y. Huang, Y. Liu et al., "Polymeric membranes incorporated with ZnO nanoparticles for membrane fouling mitigation: a brief review," *Frontiers in Chemistry*, vol. 8, 2020.

[5] L. Gamfeldt, T. Snall, R. Bagchi et al., "Higher levels of multiple ecosystem services are found in forests with more tree species," *Nature Communications*, vol. 4, 2013.

[6] Y. Xiu, N. Wang, F. X. Peng, and Q. X. Wang, "Spatial-temporal variations of water ecosystem services value and its influencing factors: a case in typical regions of the Central Loess Plateau," *Sustainability*, vol. 14, no. 12, 2022.

[7] Y. B. Li and M. J. Deng, "Spatiotemporal variations of agricultural water footprint and its economic benefits in Xinjiang, northwestern China," *Scientific Reports*, vol. 11, no. 1, 2021.

[8] F. Li, Y. M. Li, X. W. Zhou, Z. Yin, T. Liu, and Q. C. A. Xin, "Modeling and analyzing supply-demand relationships of water resources in Xinjiang from a perspective of ecosystem services," *Journal of Arid Land*, vol. 14, no. 2, pp. 115–138, 2022.

[9] Z. Chen, X. Liu, J. P. Niu et al., "Optimizing irrigation and nitrogen fertilization for seed yield in western wheatgrass [Pascopyrum smithii (Rydb.) Á. Löve] using a large multi-factorial field design," *Plos One*, vol. 14, no. 6, article e0218599, 2019.

[10] Y. X. Li, W. F. Zhang, L. Ma et al., "An analysis of China's grain production: looking back and looking forward," *Food and Energy Security*, vol. 3, no. 1, pp. 19–32, 2014.

[11] T. S. Du, S. Z. Kang, J. H. Zhang, and W. J. Davies, "Deficit irrigation and sustainable water-resource strategies in agriculture for China's food security," *Journal of Experimental Botany*, vol. 66, no. 8, pp. 2253–2269, 2015.

[12] J. J. Cheng and C. X. Xue, "The sand-damage-prevention engineering system for the railway in the desert region of the Qinghai-Tibet plateau," *Journal of Wind Engineering and Industrial Aerodynamics*, vol. 125, pp. 30–37, 2014.

[13] D. Conde, S. Solari, D. de Alava et al., "Ecological and social basis for the development of a sand barrier breaching model in Laguna de Rocha, Uruguay," *Estuarine Coastal and Shelf Science*, vol. 219, pp. 300–316, 2019.

[14] A. Musa, D. M. Jiang, and C. Y. Niu, "The applicable density of sand-fixing shrub plantation in Horqin sand land of northeastern China," *Ecological Engineering*, vol. 64, pp. 250–254, 2014.

[15] H. Katebi, A. Fahmi, H. S. Kafil, and M. H. Bonab, "Stabilization of calcareous sand dunes using phosphoric acid mulching liquid," *Journal of Arid Environments*, vol. 148, pp. 34–44, 2018.

[16] Z. J. Yi and C. H. Zhao, "Desert "soilization": an eco-mechanical solution to desertification," *Engineering*, vol. 2, no. 3, pp. 270–273, 2016.

[17] S. Z. Marandi, M. B. Salehi, and A. M. Moghadam, "Sand control: experimental performance of polyacrylamide hydrogels," *Journal of Petroleum Science and Engineering*, vol. 170, pp. 430–439, 2018.

[18] X. Zhang and H. Koehler, "Soil algae for combating soil degradation - greenhouse experiment with different soil amendments," *Soil Research*, vol. 60, pp. 1–22, 2022.

[19] T. Calver, M. Yarmuch, A. J. Conway, and K. Stewart, "Strong legacy effect of peat composition on physicochemical properties of reclamation coversoil," *Canadian Journal of Soil Science*, vol. 99, no. 3, pp. 244–253, 2019.

[20] C. San Miguel, D. Gimenez, U. Krogmann, and S. W. Yoon, "Impact of land application of cranberry processing residuals, leaves and biosolids pellets on a sandy loam soil," *Applied Soil Ecology*, vol. 53, pp. 31–38, 2012.

[21] Z. H. Sun and J. C. Han, "Effect of soft rock amendment on soil hydraulic parameters and crop performance in Mu Us sandy land, China," *Field Crops Research*, vol. 222, pp. 85–93, 2018.

[22] Y. S. Liu, X. Y. Zheng, Y. S. Wang et al., "Land consolidation engineering and modern agriculture: a case study from soil particles to agricultural systems," *Journal of Geographical Sciences*, vol. 28, no. 12, pp. 1896–1906, 2018.

[23] N. Wang, J. Xie, and J. Han, "A sand control and development model in sandy land based on mixed experiments of arsenic sandstone and sand: a case study in Mu Us sand land in China," *Chinese Geographical Science*, vol. 23, no. 6, pp. 700–707, 2013.

[24] N. Wang, J. Xie, J. Han, and L. Luo, "A comprehensive framework on land-water resources development in Mu Us sandy land," *Land Use Policy*, vol. 40, pp. 69–73, 2014.

[25] P. L. Wang, Y. Wei, F. L. Zhong, X. Y. Song, B. Wang, and Q. H. Wang, "Evaluation of agricultural water resources carrying capacity and its influencing factors: a case study of townships in the arid region of northwest China," *Agriculture-Basel*, vol. 12, no. 5, 2022.

[26] X. T. Zhu, G. P. Zhang, K. Y. Yuan, H. B. Ling, and H. L. Xu, "Evaluation of agricultural water pricing in an irrigation district based on a Bayesian network," *Water*, vol. 10, no. 6, p. 768, 2018.

[27] J. Sun, Y. P. Li, C. Suo, and J. Liu, "Development of an uncertain water-food-energy nexus model for pursuing sustainable agricultural and electric productions," *Agricultural Water Management*, vol. 241, article 106384, 2020.

[28] Z. Y. Dai and Y. P. Li, "A multistage irrigation water allocation model for agricultural land-use planning under uncertainty," *Agricultural Water Management*, vol. 129, pp. 69–79, 2013.

[29] F. Shirshahi, H. Babazadeh, N. EbrahimiPak, and M. Khaledian, "Sustainable optimization of regional agricultural water use by developing a two-level optimization model," *Arabian Journal of Geosciences*, vol. 13, no. 4, 2020.

[30] K. Malek, C. Stockle, K. Chinnayakanahalli et al., "VIC-CropSyst-v2: a regional-scale modeling platform to simulate the nexus of climate, hydrology, cropping systems, and human decisions," *Geoscientific Model Development*, vol. 10, no. 8, pp. 3059–3084, 2017.

[31] T. R. Lopes, C. A. Zolin, R. Mingoti et al., "Hydrological regime, water availability and land use/land cover change impact on the water balance in a large agriculture basin in the southern Brazilian Amazon," *Journal of South American Earth Sciences*, vol. 108, article 103224, 2021.

[32] S. Liu, N. Wang, J. Xie, R. Jiang, and M. Zhao, "A regulation-allocation coupling approach for agricultural water resources management based on water quantity orientation," *Water Supply*, vol. 21, no. 1, pp. 431–443, 2021.

[33] Y. Xue, J. Liu, P. G. Ranjith et al., "Experimental investigation of mechanical properties, impact tendency, and brittleness characteristics of coal mass under different gas adsorption pressures," *Geomechanics and Geophysics for Geo-Energy and Geo-Resources*, vol. 8, no. 5, 2022.

[34] D. Yang, W. Liu, L. Tang, L. Chen, X. Li, and X. Xu, "Estimation of water provision service for monsoon catchments of South China: applicability of the InVEST model," *Landscape and Urban Planning*, vol. 182, pp. 133–143, 2019.

[35] M. D. K. Leh, M. D. Matlock, E. C. Cummings, and L. L. Nalley, "Quantifying and mapping multiple ecosystem services change in West Africa," *Agriculture, Ecosystems & Environment*, vol. 165, pp. 6–18, 2013.

[36] M. Khan and M. K. Goyal, "Assessment of spatially explicit annual water-balance model for Sutlej River Basin in eastern Himalayas and Tungabhadra River Basin in peninsular India," *Hydrology Research*, vol. 48, no. 2, pp. 542–558, 2017.

[37] G. Cui, Y. Zhang, F. Shi et al., "Study of spatiotemporal changes and driving factors of habitat quality: a case study of the agro-pastoral ecotone in northern Shaanxi, China," *Sustainability*, vol. 14, no. 9, p. 5141, 2022.

[38] Y. Qi, Q. Chang, K. Jia, M. Liu, J. Liu, and T. Chen, "Temporal-spatial variability of desertification in an agro-pastoral transitional zone of northern Shaanxi Province, China," *Catena*, vol. 88, no. 1, pp. 37–45, 2012.

[39] B. M. Ivanovich, *Climate and Life*, Academic Press, 1974.

[40] X. Yang, R. Chen, M. E. Meadows, G. Ji, and J. Xu, "Modelling water yield with the InVEST model in a data scarce region of northwest China," *Water Supply*, vol. 20, no. 3, pp. 1035–1045, 2020.

[41] F. Baw-puh, "On the calculation of the evaporation from land surface," *Chinese Journal of Atmospheric Sciences*, vol. 5, no. 1, pp. 23–31, 1981.

[42] L. Zhang, K. Hickel, W. R. Dawes, F. H. S. Chiew, A. W. Western, and P. R. Briggs, "A rational function approach for estimating mean annual evapotranspiration," *Water Resources Research*, vol. 40, no. 2, 2004.

[43] R. J. Donohue, M. L. Roderick, and T. R. McVicar, "Roots, storms and soil pores: incorporating key ecohydrological processes into Budyko's hydrological model," *Journal of Hydrology*, vol. 436-437, pp. 35–50, 2012.

[44] A. Daneshi, R. Brouwer, A. Najafinejad, M. Panahi, A. Zarandian, and F. F. Maghsood, "Modelling the impacts of climate and land use change on water security in a semi-arid forested watershed using InVEST," *Journal of Hydrology*, vol. 593, article 125621, 2021.

[45] C. L. Li, M. Liu, Y. M. Hu, T. Shi, X. Q. Qu, and M. T. Walter, "Effects of urbanization on direct runoff characteristics in urban functional zones," *Science of the Total Environment*, vol. 643, pp. 301–311, 2018.

[46] N. Ohana-Levi, A. Givati, N. Alfasi, A. Peeters, and A. Karnieli, "Predicting the effects of urbanization on runoff after frequent rainfall events," *Journal of Land Use Science*, vol. 13, no. 1-2, pp. 81–101, 2018.

[47] X. Wang, G. Liu, D. Lin et al., "Water yield service influence by climate and land use change based on InVEST model in the monsoon hilly watershed in South China," *Geomatics, Natural Hazards and Risk*, vol. 13, no. 1, pp. 2024–2048, 2022.